ChemPubSoc Europe

DOI: 10.1002/chem.201500776

CHEMISTRY A European Journal Full Paper

Carbenes

Copper–Carbene Intermediates in the Copper-Catalyzed Functionalization of O–H Bonds

Ana Pereira,[a] Yohan Champouret,[b, c] Carmen Martín,[a] Eleuterio Álvarez,[d] Michel Etienne,*[b, c] Tomás R. Belderraín,*[a] and Pedro J. Pérez*[a]

Abstract: Copper–carbene [$Tp^xCu{=}C(Ph)(CO_2Et)$] and copper–diazo adducts [$Tp^xCu\{\eta^1\text{-}N_2C(Ph)(CO_2Et)\}$] have been detected and characterized in the context of the catalytic functionalization of O–H bonds through carbene insertion by using $N_2{=}C(Ph)(CO_2Et)$ as the carbene source. These are the first examples of these type of complexes in which the copper center bears a tridentate ligand and displays a tetrahedral geometry. The relevance of these complexes in the catalytic cycle has been assessed by NMR spectroscopy, and kinetic studies have demonstrated that the N-bound diazo adduct is a dormant species and is not en route to the formation of the copper–carbene intermediate.

Introduction

Metal-catalyzed transfer reactions of carbene from diazo compounds, $N_2CR^1R^2$, to unsaturated as well as saturated substrates constitute a powerful tool for the formation of new carbon–carbon or carbon–heteroatom bonds.[1] The particular case of a E–H bond (E = C, N, O) provides the formation of a C–E bond (Scheme 1), a moiety that is present in a plethora of natural and synthetic molecules. However, the insertion of a carbene group into such E–H bond seems to be underexploited in spite of its potential.[2] For example, inert C–H bonds of poorly reactive molecules such as alkanes,[3] including methane,[4] have been functionalized by this methodology. More reactive N–H[5] or O–H[6] bonds have also been converted into the corresponding derivatives. The asymmetric versions of those reactions with X = C,[7] N,[8] O[9] have also been reported.

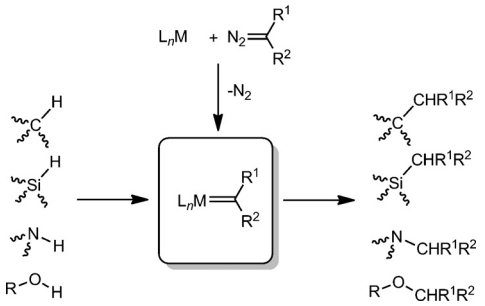

Scheme 1. General metal-catalyzed E–H functionalization by the carbene insertion methodology.

Several metals promote this transformation: rhodium, copper, iron, or ruthenium are the most frequently employed, copper being the preferred one.[2] The mechanism proposed for this transformation is shown in Scheme 2. Usually, the initial copper complex dissociates a ligand to generate a coordinatively and electronically unsaturated species that reacts with the diazo compound. There are several coordination modes for a diazo compound $N_2CR^1R^2$ with the copper center, although it has been proposed that only the complex bound through the diazo-carbon atom (**A**) is productive for the formation of the copper–carbene intermediate (**MC**). Direct observations of such species (**MC**), always in the context of olefin cyclopropanation reactions, are rare (Scheme 2).[10] In a subsequent and final step, the E–H bond interacts with the copper–carbene (**MC**) to afford the insertion product. The general catalytic cycle shown in Scheme 2 has been built[2] on the basis of evidences obtained from different systems, some of them being irrelevant to the E–H insertion reaction. With the aim of providing evidences of the different steps within the same catalytic cycle, we report herein a complete study on the reaction of

[a] *A. Pereira, Dr. C. Martín, Prof. Dr. T. R. Belderraín, Prof. Dr. P. J. Pérez*
Laboratorio de Catálisis Homogénea
Unidad Asociada al CSIC
CIQSO- Centro de Investigación en Química Sostenible
and Departamento de Química y Ciencia de Materiales
Universidad de Huelva, 21007 Huelva (Spain)
Fax: (+34) 959219942
E-mail: trodri@dqcm.uhu.es
perez@dqcm.uhu.es

[b] *Dr. Y. Champouret, Prof. Dr. M. Etienne*
CNRS; LCC (Laboratoire de Chimie de Coordination)
205, route de Narbonne, BP 44099
31077 Toulouse Cedex 4 (France)

[c] *Dr. Y. Champouret, Prof. Dr. M. Etienne*
Université de Toulouse; UPS, INPT, LCC
31077 Toulouse Cedex 4 (France)
E-mail: michel.etienne@lcc-toulouse.fr

[d] *Dr. E. Álvarez*
Instituto de Investigaciones Químicas Isla de la Cartuja
CSIC-Universidad de Sevilla
Avenida de Américo Vespucio 49
41092-Sevilla (Spain)

Supporting information for this article is available on the WWW under http://dx.doi.org/10.1002/chem.201500776.

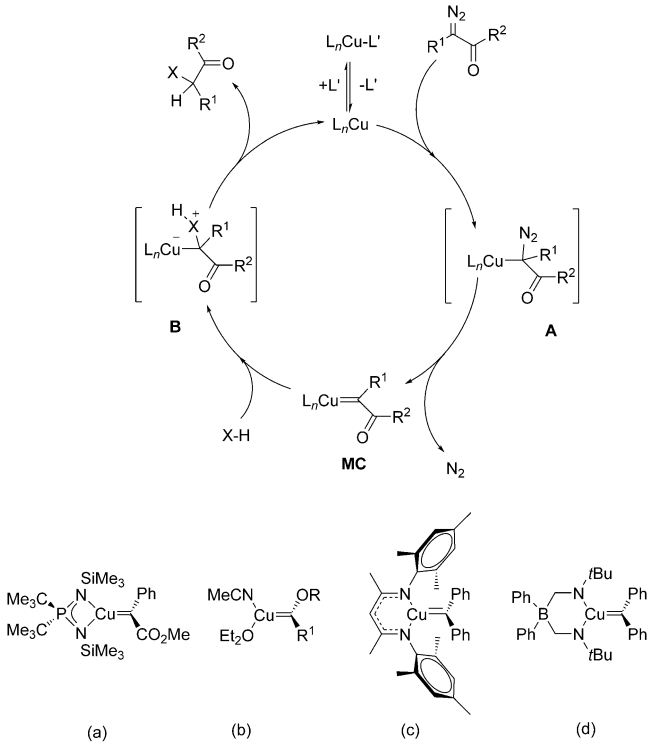

Scheme 2. Top: General catalytic cycle for the copper-catalyzed X–H insertion reaction. Bottom: The unique examples of copper–carbene intermediates relevant in carbene transfer from diazo compounds to olefins.

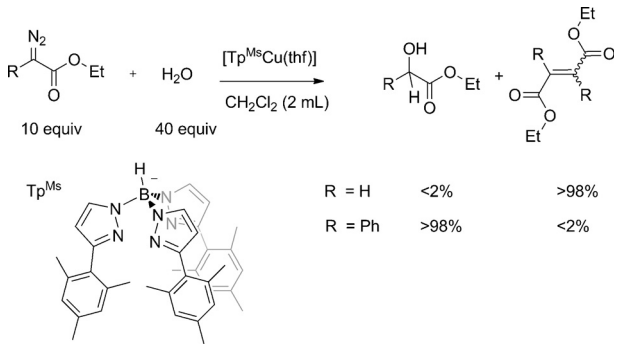

Scheme 3. Water functionalization by carbene insertion catalyzed by [Tp^{Ms}Cu(thf)]. Yields determined by using NMR spectroscopy with an internal standard.

ethyl 2-phenyldiazoacetate with water by using [Tp^{Ms}Cu(thf)] (**1**) and related [Tp^{x}Cu(L)] complexes (Scheme 3) as catalyst precursors. We successfully characterized the copper–carbene intermediate as well as the catalyst dormant species, a diazo–copper complex. NMR spectroscopy and kinetic studies have provided valuable information to build a reasonable mechanistic proposal.

Results and Discussion

Catalytic functionalization of water by carbene insertion with [Tp^{Ms}Cu(thf)] (1)

Previous works from this laboratory demonstrated the catalytic capabilities of the complex [Tp^{Ms}Cu(thf)] (**1**) for the cyclopropanation of olefins as well as the functionalization of C–H, N–H, and O–H bonds with ethyl diazoacetate (EDA) as the carbene source.[11] Interestingly, when we performed the reaction of EDA with water in the presence of catalytic amounts of **1**, the major products were diethyl fumarate and maleate, as a consequence of the catalytic dimerization of the carbene unit. The insertion product was detected in $<2\%$ yield (Scheme 3). Therefore, we chose a bulkier diazo compound such as ethyl 2-phenyldiazoacetate, $N_2C(Ph)(CO_2Et)$ (Pheda), with the aim of disfavoring this dimerization reaction. Gratifyingly, the insertion of the $C(Ph)(CO_2Et)$ unit into the O–H bond of water yielded the main product of the reaction (Scheme 3), providing a model system for our mechanistic study. The reaction was performed at room temperature and took place in 2 h.

Isolation of the diazo adduct [Tp^{Ms}Cu{η^1-N$_2$C(Ph)(CO$_2$Et)}] (2a)

Once we had demonstrated the ability of complex **1** to promote the model reaction of Pheda and H_2O, we examined the reaction of **1** with Pheda at low temperature (Scheme 4). When an equimolar mixture of both reagents in toluene was stirred at $-35\,^{\circ}C$, a smooth change in color from orange to reddish was observed, but no nitrogen evolution was noted. The addition of petroleum ether and storing at $-30\,^{\circ}C$ overnight pro-

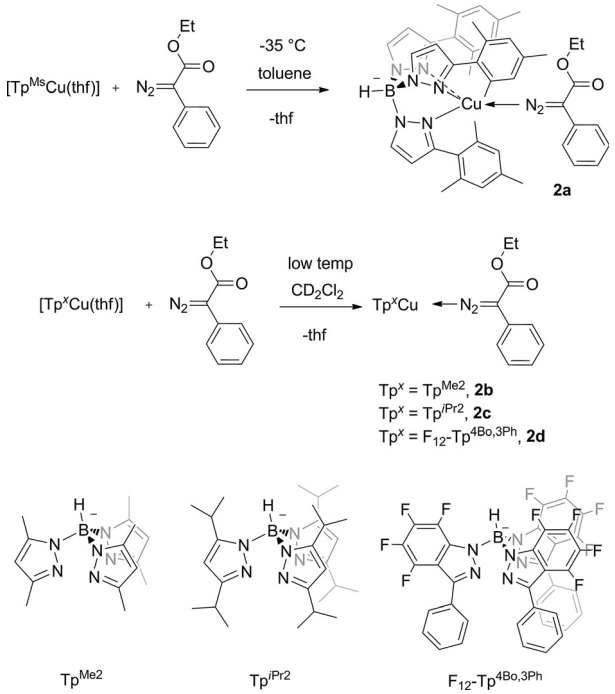

Scheme 4. Formation of the copper–diazo compound adducts **2a–d**.

vided red microcrystals of a new complex that showed absorption at 2046 cm^{-1} in the FTIR spectrum, which was due to a coordinated N_2 group (free Pheda shows this band at 2089 cm^{-1}). Multinuclear NMR data were consistent with the presence of the Tp^{Ms} ligand and a $C(Ph)CO_2Et$ moiety. The observation of a single set of resonances of the former assessed the existence of a local C_3 symmetry for **2a** in solution. The use of ^{13}C-labelled $N_2{=}^{13}C(Ph)(CO_2Et)$ gave additional information. A resonance centered at $\delta = 67.9$ ppm in the $^{13}C\{^1H\}$ NMR spectrum was assigned to the diazo carbon atom (free Pheda shows this peak at $\delta = 63.1$ ppm). On these bases, we propose that complex **2a** is formed upon coordination of Pheda to the $Tp^{Ms}Cu$ core (Scheme 4). The molecular structure of **2a** has been elucidated by using an X-ray diffraction study (Figure 1), confirming

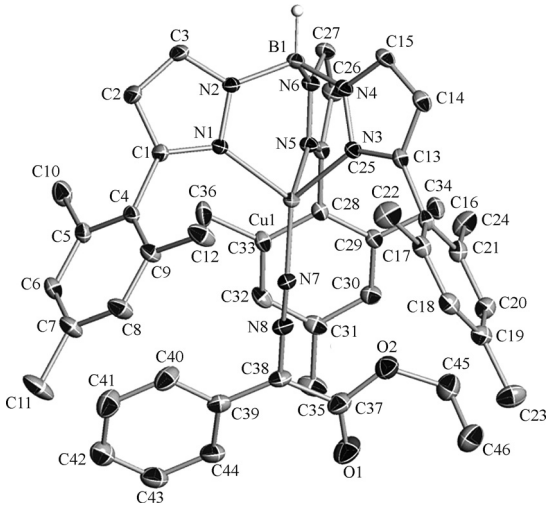

Figure 1. Molecular structure of $[Tp^{Ms}Cu\{\eta^1\text{-}N_2C(Ph)(CO_2Et)\}]$ (**2a**) (30% displacement ellipsoids; hydrogen atoms have been omitted except for the one bound to the boron atom).

our proposal: Complex $Tp^{Ms}Cu[\eta^1\text{-}N_2C(Ph)(CO_2Et)]$ contains the diazo compound bound to the metal center in a terminal fashion.

Examples of copper(I) diazo compound adducts with the diazo functionality bonded in a η^1-fashion are scarce. To the best of our knowledge, there are only two examples in which the copper is supported by a bis(phosphino)borate ligand: $[Ph_2B(CH_2PtBu_2)_2]Cu([\eta^1\text{-}N_2C(SiMe_3)_2]$ and $Ph_2B(CH_2PtBu_2)_2]Cu([\eta^1\text{-}N_2CMes_2]$. Geometry around the metal center is trigonal planar, at variance with that in **2a**, in which the κ^3 coordination of the Tp^{Ms} ligand ensures a tetrahedral geometry. Therefore, complex **2a** is the first example of a η^1-*N*-diazo compound adduct in such an environment. The Pheda ligand behaves as a σ-donor ligand without significant contribution of π-back-bonding from the metal to the diazoalkane ligand,[12] as inferred from the structural data: the N(7)-N(8) [1.1371(18) Å] and N(8)-C(38) [1.322(2) Å] bond lengths and the N(7)-N(8)-C(38) angle [178.59(17)°] for **2a** are comparable to the corresponding values found for free phenyldiazoacetates, a feature also observed in the trigonal planar complexes mentioned above. As for $[\{Ph_2B(CH_2PtBu_2)_2\}Cu\{\eta^1\text{-}N_2CMes_2\}]$, the N(8)-N(7)-Cu(1) angle slightly deviates from linearity [161.17(13)°]. Nevertheless, these data show that both N(7) and N(8) present sp hybridization (see the Supporting Information for full description of the crystal structure).

Three other copper–diazo adducts have been generated in situ upon the direct reaction of $N_2{=}^{13}C(Ph)(CO_2Et)$ with the complexes $[Tp^{iPr2}Cu(CH_3CN)]$, $[(Tp^*Cu)_2]$ and $[(F_{12}\text{-}Tp^{4Bo,3Ph})Cu(acetone)]$ (Scheme 4). The new complexes $[Tp^xCu\{\eta^1\text{-}N_2{}^{13}C(Ph)(CO_2Et)\}]$ ($Tp^x = Tp^{Me2}$, **2b**; Tp^{iPr2}, **2c**; $F_{12}\text{-}Tp^{4Bo,3Ph}$, **2d**) were detected in solution below room temperature by using $^{13}C\{^1H\}$ NMR spectroscopy showing the resonances of the diazo carbon at $\delta = 67.7$, 67.3, and 66.9 ppm, respectively. These compounds will be of interest in the generation of the copper–carbenes described below.

In situ generation and characterization of the copper carbene complexes $[Tp^xCu{=}C(Ph)(CO_2Et)]$ (3)

When a CH_2Cl_2 solution of **1** and 3 equiv of Pheda prepared at −30 °C was allowed to reach room temperature, the color changed from reddish to dark brown and then to dark orange. NMR studies of the final mixture showed a combination of products including 1) $(Ph)(OH)CH(CO_2Et)$ resulting from the insertion of the $C(Ph)(CO_2Et)$ unit into the O–H bond of adventitious water, 2) the olefins resulting from carbene coupling, *E*- and *Z*-$(Ph)(CO_2Et)C{=}C(Ph)(CO_2Et)$, and 3) the azine $EtO_2C(Ph)C{=}N{-}N{=}C(Ph)CO_2Et$ (Scheme 5).[13] Monitoring the reaction by

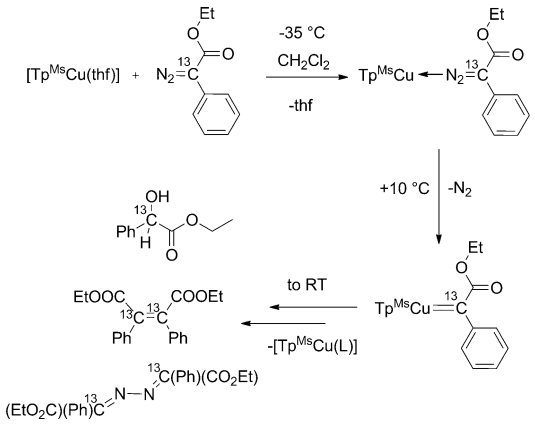

Scheme 5. The reaction of Pheda and complex **1** and the different species observed by $^{13}C\{^1H\}$ NMR spectroscopy at different temperatures.

using $^{13}C\{^1H\}$ NMR spectroscopy in CD_2Cl_2 showed that at −40 °C only the resonances assigned to the diazo adduct **2a** (^{13}C-enriched) were observed. The temperature was then progressively increased and, at +10 °C, a new resonance raised at $\delta = 248.5$ ppm, which was assigned to the carbene carbon of the complex $[Tp^{Ms}Cu{=}^{13}C(Ph)(CO_2Et)]$ (**3a**) on the basis of the previously described copper carbenes by the groups of Hofmann (Scheme 2a, $\delta = 229.9$ ppm),[10a] Barluenga (Scheme 2b, $\delta = 276.5$ ppm),[10b] and Warren (Scheme 2c, $\delta = 253.1$ ppm).[10b] Above that temperature, reactions with adventitious water or the free diazo compound took place leading to the aforemen-

tioned mixture of products. Other resonances of the Tp^{Ms} ligand and C(Ph)(CO_2Et) fragment were also observed (see the Supporting Information).

The observation of the carbenic resonance was not exclusive of the Tp^{Ms}-containing copper complex. Following the same procedure, the three other Tp^xCu complexes (see Scheme 4) behaved similarly leading to the formation of the corresponding copper–carbene complexes [$Tp^xCu{=}^{13}C(Ph)(CO_2Et)$] ($Tp^x$ = Tp^{Me2}, **3b**; Tp^{iPr2}, **3c**; F_{12}-$Tp^{4Bo,3Ph}$, **3d**). Figure 2 shows the

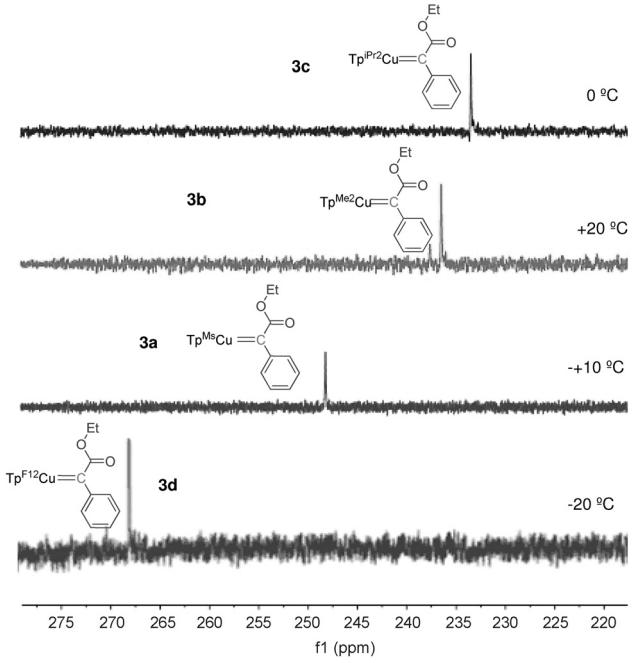

Figure 2. ^{13}C NMR region for the carbene carbon resonances of complexes **3a–d**.

downfield region of the ^{13}C NMR spectra in which the carbenic carbon resonates (^{13}C-labelled Pheda was employed in all cases). The chemical shift increased in the order $Tp^{iPr2} < Tp^{Me2} < Tp^{Ms} < F_{12}$-$Tp^{4Bo,3Ph}$. Interestingly, we have found that there is a good linear correlation between the values of ν(CO) of the [Tp^xCu(CO)] complexes and the chemical shift of the carbenic carbon (Table 1 and Figure 3). Thus, a decrease of electron density at the metal center when using poorly donating Tp^x ligands induces a deshielding of the carbene carbon and, consequently, the corresponding peak appears at higher frequency. This is reminiscent of the related nature of the M–CO and M–CR_2 bonding, with σ donation from the ligand to the metal and π back-donation from the metal to the ligand (Figure 4).

Table 1. Values of ν(CO)[14] in [Tp^xCu(CO)] and $\delta C_{carbene}$ in complexes **3a–d**.

Tp^x Ligand	ν(CO) in [Tp^xCu(CO)] [cm^{-1}]	$\delta C_{carbene}$ [ppm]
Tp^{iPr2}	2056	233.9
Tp*	2060	236.8
Tp^{Ms}	2079	248.5
F_{12}-$Tp^{4Bo,3Ph}$	2113	268.4

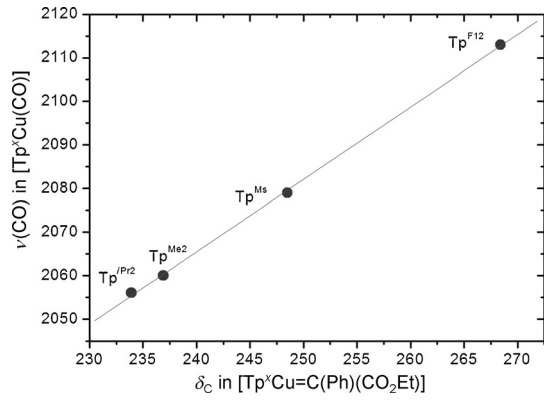

Figure 3. Plot of the chemical shift of the carbene atom in complexes **3a–d** versus the ν(CO) value in the corresponding [Tp^xCu(CO)].

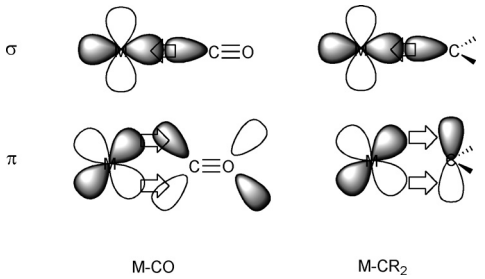

Figure 4. A simplified comparison of the bonding of the M–CO and M–CR_2 moieties.

The nature of the Tp^x ligand affects the electron density at the metal center in the much same way in both cases.

It is the first time that four-coordinate tetrahedral copper–carbene complexes such as **3a–d** have been detected; previous examples (see Scheme 2)[10] are reduced to trigonal planar geometries with bi- or monodentate ancillary ligands. However, attempts to grow single crystals of **3a–d** suitable for X-ray diffraction study proved unsuccessful because of the poor stabilities of these complexes.

Kinetic studies of the reaction of Pheda and H_2O catalyzed by [Tp^{Ms}Cu(thf)] (1)

We have carried out kinetic studies based on the measurement of the evolution of dinitrogen during the catalytic reaction of Pheda and H_2O by using **1** as the catalyst precursor. When a 1:10:90 mixture of **1**/Pheda/H_2O (referred to 0.01 mmol of **1**) was reacted at 25 °C, a smooth reaction took place in which gas evolution was detected (see the Supporting Information for technical details) as shown in Figure 5. Fitting the experimental data into an exponential growth function led to the value of k_{obs} for this experiment. With this methodology, we have performed a series of experiments in which the relative amounts of catalyst, Pheda, H_2O, and temperature have been varied. Table 2 contains all the collected data, from which some trends can be extracted. First, Pheda inhibits the reaction as the rate decreases when the concentration of Pheda increases (Table 2, entries 1–3); we suggest this is the result of

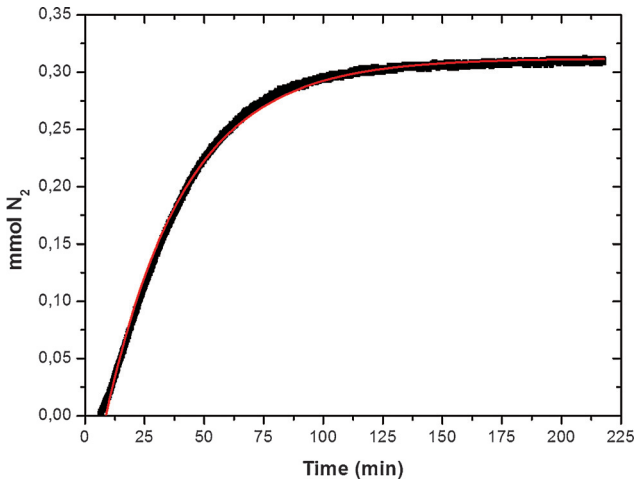

Figure 5. Nitrogen evolution in the reaction of Pheda and H_2O using [Tp^{Ms}Cu(thf)] (**1**) as the catalyst.

Table 2. Kinetic experiments of the reaction of Pheda and H_2O using [Tp^{Ms}Cu(thf)] (**1**) as the catalyst.[a]

Entry	**1** [equiv][b]	Pheda [equiv]	H_2O [equiv]	T [K]	k_{obs} [min^{-1}]
1	1	10	90	298	$6.27(2)\times10^{-4}$
2	1	30	90	298	$5.04(9)\times10^{-4}$
3	1	60	90	298	$3.96(2)\times10^{-4}$
4	1	30	180	298	$4.40(6)\times10^{-4}$
5	1	30	270	298	$4.59(6)\times10^{-4}$
6	1	10	40	278	$8.82(9)\times10^{-5}$
7	1	10	40	288	$2.77(6)\times10^{-4}$
8	1	10	40	298	$3.77(3)\times10^{-4}$
9	1	10	40	308	$5.41(2)\times10^{-4}$

[a] See the Supporting Information for the experimental details. [b] Refers to 0.01 mmol of catalyst.

the formation of the diazo adduct **2a**. Secondly, the variation of [H_2O] does not seem to have any influence on the nitrogen evolution (Table 2, entries 2, 4, and 5). Therefore, dinitrogen extrusion and copper–carbene formation must occur prior to any interaction with water, as expected. More interestingly, this also demonstrates that the formation of the [Tp^{Ms}Cu(OH_2)] adduct is not favored, otherwise the amount of active copper species would be reduced and the reaction rate affected by [H_2O].

The effect of the temperature on this transformation has also been studied (Table 2, entries 6–9), leading to the Eyring plot shown in Figure 6, from which the activation parameters have been obtained. $\Delta H^{\neq}$ and $\Delta S^{\neq}$ were determined as 10.3(1) kcal mol^{-1} and −47.4(4) cal mol^{-1} K^{-1}, respectively, pointing to an associative nature of the key step in the catalytic cycle. The negative value of activation entropy finds precedents in the literature. Kochi and Salomon reported a value of $\Delta S^{\neq} = -8.90$ cal mol^{-1} K^{-1} for the cyclopropanation of 1-hexene with EDA catalyzed by Cu^{I}OTf, although such value was attributed to the coordination of the olefin.[15] Warren and co-workers described similar values for the reaction of the copper–carbene [(NN)Cu=CPh_2] with styrene.[10c] Alonso and García determined[16] the kinetic parameters for the rhodium acetate-catalyzed C–H insertion reaction of EDA into dioxane and postulated that the large negative entropy of activation (−25 cal mol^{-1} K^{-1}) for this reaction could be attributed to a rate-determining step that would not involve dinitrogen loss along the lines we observe here. Regarding the $\Delta H^{\neq}$ value of 10.3(1) kcal mol^{-1}, the mentioned previous work provided similar values (16.4[16] and 19.1[15] kcal mol^{-1}].

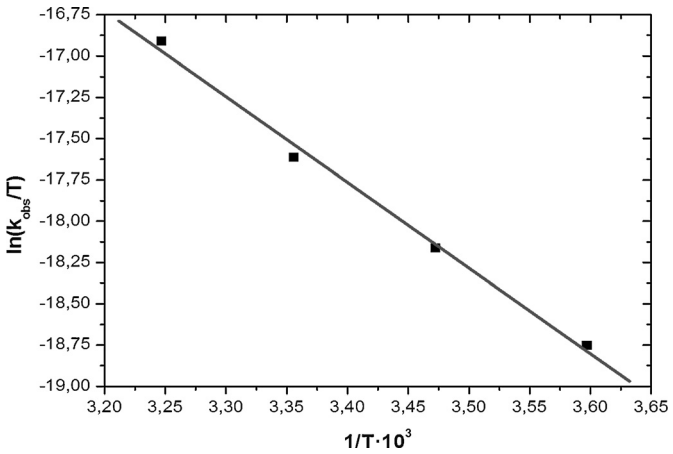

Figure 6. Eyring plot for the reaction of Pheda and H_2O using [Tp^{Ms}Cu(thf)] (**1**) as the catalyst.

We have also employed the isolated copper diazo adduct **2a** to monitor dinitrogen evolution. When a solution of **2a** in CD_2Cl_2 ([**2a**] = 7.8×10^{-3} M) was stirred at 5 °C, dinitrogen evolution was observed immediately, and ceased after 4–5 min (see the Supporting Information for kinetic curves). NMR studies of the reaction mixture revealed the formation of the product resulting from insertion of the carbene in the O–H bond of water in the purposely wet solvent. A small amount of free diazo compound that co-crystallized with complex **2a** was quantified as 15% relative to the copper complex. In spite of that, the reaction was quite fast; a larger amount of Pheda being required to slow down the reaction rate, because it occurs under catalytic conditions. The experimental data support the proposal of **2a** being the catalyst resting state, yet acting as a dormant species. It is the dissociation equilibrium **2a**–**4** that regulates the amount of [Tp^{Ms}Cu] (**4**) delivered into the catalytic cycle to effectively promote the O–H functionalization.

Mechanistic proposal

On the basis of the collected data, an overall mechanistic picture can be built, as shown in Scheme 6. The catalyst precursor **1** readily dissociates the thf ligand to generate an unsaturated [Tp^{Ms}Cu] (**4**) intermediate that is trapped by Pheda to afford the adduct **2a**. The intermediate **4**, similar to other species that have been postulated by means of DFT calculations,[17] can coordinate the diazo reagent by the diazo carbon atom leading to **5**. This is very likely a less favorable process than the former; if not, the dinitrogen evolution would be accelerated when increasing [Pheda], opposite to the experimental observation. In the absence of free Pheda, H_2O functionalization is fast, implying that the equilibria between **2a**, **4**, and **5** ensures

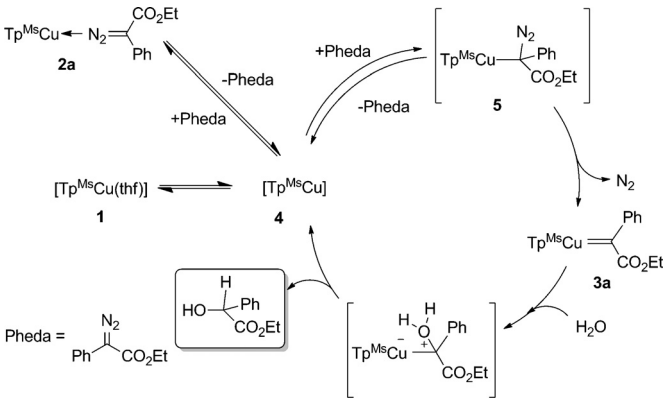

Scheme 6. The catalytic cycle of the $Tp^{Ms}Cu$-catalyzed OH functionalization by carbene insertion with N_2=C(Ph)(CO_2Et).

enough amount of the latter to generate the copper–carbene **3a**. Recall that **3a** is quantitatively generated in situ with just 3 equiv of Pheda related to **1**. The observation of a negative value of the activation entropy can be explained in terms of the formation of **5** from **4**.

The final step of the interaction of the copper–carbene **3a** with H_2O would be the electrophilic attack of the carbene ligand to the oxygen atom, generating an ylidic-type of intermediate, from which the product would evolve. The formation of such species in several Tp^xCu-catalyzed carbene transfer reactions involving heteroatoms have been invoked from DFT calculations.[18] It has also been proposed[19] that the process might occur with the intermediacy of more than one molecule of H_2O, although at this stage we have not obtained any evidence for that in our system.

Conclusion

We have studied the catalytic functionalization of the O–H bond of H_2O by using the copper–catalyzed transfer and insertion of a carbene C(Ph)(CO_2Et) group with N_2C(Ph)(CO_2Et) as the carbene source, and the complex [Tp^{Ms}Cu(thf)] (**1**). The presence of a four-coordinate tetrahedral copper–carbene intermediate [Tp^xCu=C(Ph)(CO_2Et)] has been demonstrated. The diazo complex [Tp^{Ms}Cu{η^1-N_2=C(Ph)(CO_2Et)}] has been isolated and structurally characterized. Kinetic studies have shown that this compound is a dormant species and constitutes the resting state of the catalyst in this system.

Experimental Section

General methods

All reactions and manipulations were carried out under a dinitrogen or argon atmosphere by using standard Schlenk techniques or under nitrogen or argon atmosphere in an Mbraun or Jacomex glovebox, respectively. All substrates were purchased from Aldrich and used without further purification. Solvents were distilled and degassed before use. The diazo compound N_2C(Ph)(CO_2Et),[20] including the ^{13}C-labelled sample, the homoscorpionate ligands (Tp^{Ms}, Tp*, Tp^{iPr2}, and F_{12}-$Tp^{4Bo,3Ph}$)[21] as well as their complexes[14] were prepared according to the literature methods. The synthesis of the new complex **1d** is described below. NMR spectra were recorded on Agilent 400 MR, Agilent 500 DD2, Bruker Avance 300, 400, or 500 spectrometers. FTIR spectra were recorded on a Nicolet IR200 FTIR spectrometer. ^{1}H and ^{13}C NMR shifts were measured relative to deuterated solvents peaks but are reported relative to tetramethylsilane. ^{19}F NMR chemical shifts are reported relative to external $CFCl_3$. Elemental analyses were performed on a PerkinElmer Series II CHNS/O Analyzer 2400. Dinitrogen evolution was recorded using a Man on the Moon Tech X201 Kinetic Kit.

Syntheses

Tp^{Ms}Cu[η^1-N_2C(Ph)(CO_2Et)] (2a): The complex [Tp^{Ms}Cu(thf)] (0.14 mmol) was dissolved in toluene (5 mL) in a Schlenk tube. Ethyl 2-diazo-2-phenyl acetate (0.14 mmol) was added at −35 °C. The reaction was stirred at −35 °C for 1 h. Complex **2a** was isolated as a red solid from toluene/petroleum ether (1:2) at −30 °C. ^{1}H NMR (500 MHz, −40 °C, CD_2Cl_2): δ = 1.26 (t, J = 7.1 Hz, 3H, OCH_2CH_3),1.88 (s, 18H, CH_3), 2.04 (s, 9H, CH_3), 4.15 (q, J = 6.9 Hz, 2H, OCH_2CH_3), 6.08 (br s,3H, $CH_{pyrazol}$), 6.63 (br s, 6H, $CH_{mesityl}$), 7.16 (m, 3H, CH_{phenyl}), 7.23 (t, J = 7.3 Hz, 2H, CH_{phenyl}), 7.82 ppm (br s, 3H, $CH_{pyrazol}$); ^{13}C{^{1}H} NMR (125 MHz, −40 °C, CD_2Cl_2): δ = 15.1 (OCH_2CH_3), 20.4 ($CH_{3mesityl}$), 21.0 ($CH_{3mesityl}$), 60.6 (OCH_2), 105.0 ($CH_{pyrazol}$), 128.2 ($CH_{mesityl}$), 125.3 (CH_{phenyl}), 128.5 (CH_{phenyl}), 129.0 (CH_{phenyl}), 130.3 ($C_{qmesityl}$), 135.0 ($CH_{pyrazol}$), 136.9 ($Cq_{mesityl}$), 137.4 ($Cq_{mesityl}$), 138.1 ($C_{qpyrazol}$), 150.8 (C_{phenyl}), 163.2 ppm (C=O); IR (KBr): $\tilde{\nu}$ = 2046 (νN_2) cm^{-1}.

F_{12}-$Tp^{4Bo,3Ph}$Cu(acetone) (1d): Tl(F_{12}-$Tp^{4Bo,3Ph}$)[21d] (0.505 mg, 0.5 mmol) and CuI (0.114 mg, 0.6 mmol) were placed in a Schlenk flask and acetone (25 mL) was added under stirring. After stirring overnight, the solvent was removed under vacuum to afford a yellow solid. The yellow solid was then placed in CH_2Cl_2 (10 mL), filtered over Celite, and the solvent was removed under vacuum. The solid was crystallized from dichloromethane at −25 °C to give colorless microcrystalline solid of F_{12}-$Tp^{4Bo,3Ph}$Cu(acetone) (**1d**) (140 mg, 30%). ^{1}H NMR (500 MHz, 25 °C, CD_2Cl_2): δ = 1.74 (s, 6H, CH_3COCH_3), 7.48–7.72 (m, 15H, 3 CH_{phenyl}). ^{13}C{^{1}H} NMR (125 MHz, 25 °C, CD_2Cl_2): δ = 30.2 (CH_3COCH_3), 108.5 (d, J = 16 Hz, $C_{indazol}$), 128.2 (C_{phenyl}), 129.2 (C_{phenyl}), 129.5 (C_{phenyl}), 131.0 (m, $C_{indazol}$), 131.3 (C_{phenyl}), 134.4 (dd, J = 250, 10 Hz, $CF_{indazol}$), 134.8 (ddd, J = 243, 16, 15 Hz, $CF_{indazol}$), 139.0 (dd, J = 256, 11 Hz, $CF_{indazol}$), 140.5 (ddd, J = 247, 16, 15 Hz, $CF_{indazol}$), 145.1 ppm ($C_{indazol}$). The ^{13}C peak of the carbonyl of acetone could not be detected. ^{19}F NMR (282 MHz, 25 °C, CD_2Cl_2): δ = −166.8 (t, J = 20 Hz, $CF_{indazol}$), −157.6 (t, J = 20 Hz, $CF_{indazol}$), −153.3 (m, $CF_{indazol}$), −146.0 ppm (t, J = 20 Hz, $CF_{indazol}$); elemental analysis calcd (%) for $C_{42}H_{22}BCuF_{12}N_6O$ (929.02 g mol^{-1}): C 54.30, H 2.39, N 9.05; found: C 54.09, H 2.00, N 9.00.

Reaction of Tp^{Ms}Cu(thf) and ^{13}C-labeled ethyl 2-diazo-2-phenylacetate: Detection of [Tp^{Ms}Cu{η^1-N_2-^{13}C(Ph)(CO_2Et)}] (2a) and [Tp^{Ms}Cu=^{13}C(Ph)(COOEt)] (3a): A solution of [Tp^{Ms}Cu(thf)] (12 mg, 0.017 mmol) in CD_2Cl_2 (0.5 mL) was transferred to a NMR tube that was sealed with a Teflon stopper and was cooled at −40 °C. 140 μL of a stock solution of the diazo compound and $^{13}C_2$-labelled ethyl 2-diazo-2-phenylacetate (0.35 M in CD_2Cl_2) were then added. The reaction mixture was monitored by using NMR spectroscopy from −40 to +10 °C. Selected peaks in the ^{13}C{^{1}H} NMR spectrum of the reaction mixture (125 MHz, CD_2Cl_2): At −40 °C, δ = 67.9 ppm (N_2^{13}C) for **2a**; at +10 °C, δ = 248.5 (Cu=^{13}C) for **3a**, 162.5 [azine, (EtO_2C)(Ph)^{13}C=N–N=^{13}C(Ph)(CO_2Et)], 137.3 (diethyl 2,3-diphenylmaleate, ^{13}C=^{13}C), 72.7 ppm (ethyl mandelate,^{13}CH=OH). The same procedure was applied with the other Tp^xCu complexes to observe the copper–carbenes **3b–d**. See the Supporting Information for spectra and details.

Kinetic studies on the carbene insertion into O–H bond using Pheda as the diazo compound and [Tp^{Ms}Cu(thf)] (1) as the catalyst precursor: Nitrogen evolution measurements were performed by using a device consisting of a stainless-steel gas reservoir doubly connected to a pressure transmitter, and an electronic pressure meter/controller (EL-Press, Bronkhorst HI-TEC). The outlet of the pressure controller was connected to a 100 mL reaction flask, also connected to a Schlenk manifold to allow for manipulation of the reaction and degassing. The N_2 pressure increase was measured after addition of Pheda (0.1 mmol) to a stirred solution of H_2O (0.4 mmol) and [Tp^{Ms}Cu(thf)] (0.01 mmol) in CH_2Cl_2 (2 mL) at a fixed temperature. The mixture appeared homogenous in all cases. See the Supporting Information for technical details.

Crystal X-ray structure analysis for 2a

Crystal of suitable of size for X-ray diffraction analysis was coated with dry perfluoropolyether and mounted on glass fibers and fixed in a cold nitrogen stream ($T = 100$ K) to the goniometer head. Data collection was performed on a Bruker-Nonius X8 Apex-II CCD diffractometer, using monochromatic radiation $\lambda(Mo_{K\alpha}) = 0.71073$ Å, by means of ω and ϕ scans with a width of 0.50 degree. The data were reduced (SAINT)[22] and corrected for absorption effects by the multi-scan method (SADABS).[23] The structures were solved by direct methods (SIR-2002)[24] and refined against all F^2 data by full-matrix least-squares techniques (SHELXTL-6.12)[25] minimizing $w[F_o^2 - F_c^2]^2$. All the non-hydrogen atoms were refined anisotropically. The hydrogen atoms were placed in geometrically calculated positions using a riding model.

CCDC 1045503 contains the supplementary crystallographic data for this paper. These data can be obtained free of charge from The Cambridge Crystallographic Data Centre via www.ccdc.cam.ac.uk/data_request/cif.

Acknowledgements

Support for this work was provided by the MINECO (CTQ2011-28942-CO2-01, CTQ2014-52769-C3-1-R and CTQ2011-24502) and the Junta de Andalucía (P10-FQM-06292). A.P. thanks MEC for FPU fellowship. Y.C. and M.E. thank the Institut de Chimie of the CNRS for support. Dr. Christian Bijani (LCC) is acknowledged for the low-temperature NMR studies.

Keywords: carbenes · copper · diazo compounds · ligands · NMR spectroscopy

[1] a) T. Ye, M. A. McKervey, *Chem. Rev.* **1994**, *94*, 1091 – 1160; b) M. P. Doyle, T. Ye, M. A. McKervey, *Modern Catalytic Methods for Organic Synthesis with Diazo Compounds*, Wiley, New York, **1998**; c) M. P. Doyle, R. Duffy, M. Ratnikov, *Chem. Rev.* **2010**, *110*, 704 – 724.

[2] D. Gillingham, N. Fei, *Chem. Soc. Rev.* **2013**, *42*, 4918 – 4931.

[3] a) M. M. Diaz-Requejo, A. Caballero, M. R. Fructos, P. J. Pérez in *Alkane C-H Activation by Single-Site Metal Catalysis* (Ed.: P. J. Pérez), Springer, Amsterdam, **2012**, Chapter 6; b) M. M. Díaz-Requejo, P. J. Pérez, *Chem. Rev.* **2008**, *108*, 3379 – 3394; c) M. M. Díaz-Requejo, T. R. Belderraín, M. C. Nicasio, P. J. Pérez, *Dalton Trans.* **2006**, 5559 – 5566.

[4] A. Caballero, E. Despagnet-Ayoub, M. M. Díaz-Requejo, A. Díaz-Rodríguez, M. E. González-Núñez, R. Mello, B. K. Muñoz, W. Solo Ojo, G. Asensio, M. Etienne, P. J. Pérez, *Science* **2011**, *332*, 835 – 838.

[5] a) M. Yang, X. Wang, H. Li, P. Livant, *J. Org. Chem.* **2001**, *66*, 6729 – 6733; b) M. E. Morilla, M. M. Díaz-Requejo, T. R. Belderrain, M. C. Nicasio, S. Trofimenko, P. J. Pérez, *Chem. Commun.* **2002**, 2998 – 2999; c) M. L. Kantam, B. Neelima, C. V. Reddy, *J. Mol. Catal. A* **2006**, *256*, 269 – 272; d) L. K. Baumann, H. M. Mbuvi, G. Mbuvi, G. Du, L. K. Woo, *Organometallics* **2007**, *26*, 3995 – 4002; e) P. Le Maux, I. Nicolas, S. Chevance, G. Simonneaux, *Tetrahedron* **2010**, *66*, 4462 – 4468.

[6] a) A. F. Noels, A. Demonceau, N. Petiniot, A. Hubert, P. Teyssie, *Tetrahedron* **1982**, *38*, 2733 – 2739; b) D. J. Miller, C. J. Moody, *Tetrahedron* **1995**, *51*, 10811 – 10843.

[7] a) H. M. L. Davies, T. Hansen, M. R. Churchill, *J. Am. Chem. Soc.* **2000**, *122*, 3063 – 3070; b) H.-Y. Thu, G.-M. Tong, J.-S. Huang, S. L.-F. Chan, Q.-H. Deng, C.-M. Che, *Angew. Chem. Int. Ed.* **2008**, *47*, 9747 – 9751; *Angew. Chem.* **2008**, *120*, 9893 – 9897.

[8] a) S. Bachmann, D. Fielenbach, K. A. Jørgensen, *Org. Biomol. Chem.* **2004**, *2*, 3044 – 3049; b) B. Liu, S. F. Zhu, W. Z. C. Chen, Q. L. Zhou, *J. Am. Chem. Soc.* **2007**, *129*, 5834 – 5835; c) B. Xu, S. F. Zhu, X. L. Xie, J. J. Shen, Q. L. Zhou, *Angew. Chem. Int. Ed.* **2011**, *50*, 11483 – 11486; *Angew. Chem.* **2011**, *123*, 11685 – 11688.

[9] a) T. C. Maier, G. C. Fu, *J. Am. Chem. Soc.* **2006**, *128*, 4594 – 4595; b) S.-F. Zhu, Y. C. C. Chen, Q.-L. Zhou, *Angew. Chem. Int. Ed.* **2008**, *47*, 932 – 934; *Angew. Chem.* **2008**, *120*, 946 – 948.

[10] a) B. F. Straub, P. Hofmann, *Angew. Chem. Int. Ed.* **2001**, *40*, 1288 – 1290; *Angew. Chem.* **2001**, *113*, 1328 – 1330; b) J. Barluenga, L. A. López, O. Löber, M. Tomás, S. García-Granda, C. Álvarez-Rúa, J. Borge, *Angew. Chem. Int. Ed.* **2001**, *40*, 3392 – 3394; *Angew. Chem.* **2001**, *113*, 3495 – 3497; c) X. L. Dai, T. H. Warren, *J. Am. Chem. Soc.* **2004**, *126*, 10085 – 10094; d) N. Mankad, J. N. Peters, *Chem. Commun.* **2008**, 1061 – 1063.

[11] a) M. M. Díaz-Requejo, A. Caballero, T. R. Belderrain, M. C. Nicasio, S. Trofimenko, P. J. Pérez, *J. Am. Chem. Soc.* **2002**, *124*, 978 – 983; b) M. M. Díaz-Requejo, T. R. Belderrain, M. C. Nicasio, S. Trofimenko, P. J. Pérez, *J. Am. Chem. Soc.* **2002**, *124*, 896 – 897; c) M. E. Morilla, M. J. Molina, M. M. Díaz-Requejo, T. R. Belderrain, M. C. Nicasio, S. Trofimenko, P. J. Pérez, *Organometallics* **2003**, *22*, 2914 – 2918.

[12] J. Egloff, M. Ranocchiari, A. Schira, C. Schotes, A. Mezzetti, *Organometallics* **2013**, *32*, 4690 – 4701, and references therein.

[13] Previous work from our laboratory proposed mechanistic pathways leading to the carbene coupling and azine formation; see: I. Rivilla, W. M. C. Sameera, E. Alvarez, M. M. Díaz-Requejo, F. Maseras, P. J. Pérez, *Dalton Trans.* **2013**, *42*, 4132 – 4138.

[14] a) C. Mealli, C. S. Arcus, J. L. Wilkinson, T. J. Marks, J. A. Ibers, *J. Am. Chem. Soc.* **1976**, *98*, 711 – 718; b) J. L. Schneider, S. M. Carrier, C. E. Ruggiero, V. G. Young, W. B. Tolman, *J. Am. Chem. Soc.* **1998**, *120*, 11408 – 11418; c) K. Fujisawa, T. Ono, Y. Ishikawa, N. Amir, Y. Miyashita, K.-I. Okamoto, N. Lehnert, *Inorg. Chem.* **2006**, *45*, 1698 – 1713; d) see the Supporting Information.

[15] R. G. Salomon, J. K. Kochi, *J. Am. Chem. Soc.* **1973**, *95*, 3300 – 3310.

[16] M. E. Alonso, M. C. García, *Tetrahedron* **1989**, *45*, 69 – 76.

[17] See, for example: J. M. Muñoz-Molina, W. M. C. Sameera, E. Álvarez, F. Maseras, T. R. Belderraín, P. J. Pérez, *Inorg. Chem.* **2011**, *50*, 2458 – 2467.

[18] a) J. Urbano, A. A. C. Braga, F. Maseras, E. Álvarez, M. M. Díaz-Requejo, P. J. Pérez, *Organometallics* **2009**, *28*, 5968 – 5981; b) M. Corro, M. Besora, C. Maya, E. Álvarez, J. Urbano, M. R. Fructos, F. Maseras, P. J. Pérez, *ACS Catal.* **2014**, *4*, 4215 – 4222.

[19] Y. Liang, H. Zhou, Z.-X. Yu, *J. Am. Chem. Soc.* **2009**, *131*, 17783 – 17785.

[20] a) M. Ranocchiari, A. Mezzetti, *Organometallics* **2009**, *28*, 3611 – 3613; b) C. Peng, J. Cheng, J. Wang, *J. Am. Chem. Soc.* **2007**, *129*, 8708 – 8709.

[21] a) Tp^{Ms}: A. L. Rheingold, C. B. White, S. Trofimenko, *Inorg. Chem.* **1993**, *32*, 3471 – 3477; b) Tp*: S. Trofimenko, *J. Am. Chem. Soc.* **1967**, *89*, 3170 – 3177; c) Tp^{iPr2}: N. Kitajima, K. Fujisawa, C. Fujimoto, Y. Moro-oka, S. Hashimoto, T. Kitagawa, K. Toriumi, K. Tatsumi, A. Nakamura, *J. Am. Chem. Soc.* **1992**, *114*, 1277 – 1291; d) F_{12}-Tp^{4Bo,3Ph}: W.-S. Ojo, K. Jacob, E. Despagnet-Ayoub, B. K. Muñoz, S. Gonell, L. Vendier, V.-H. Nguyen, M. Etienne, *Inorg. Chem.* **2012**, *51*, 2893 – 2901.

[22] Bruker (**2007**), *APEX2*, Bruker AXS Inc., Madison, Wisconsin, USA.

[23] Bruker (**2001**), *APEX2*, Bruker AXS Inc., Madison, Wisconsin, USA.

[24] C. M. Burla, M. Camalli, B. Carrozzini, G. L. Cascarano, C. Giacovazzo, G. Poliori, R. Spagna, *J. Appl. Cryst.* **2003**, *36*, 1103.

[25] G. M. Sheldrick, *Acta Crystallogr. Sect. A* **2008**, *64*, 112 – 122.

Received: February 26, 2015
Published online on May 26, 2015